Power Quality Assessment and Event Detection in Distribution Network with Wind Energy Penetration Using Stockwell Transform and Fuzzy Clustering

Om Prakash Mahela, Baseem Khan, Hassan Haes Alhelou, *Member, IEEE*, Pierluigi Siano, *Senior Member, IEEE*

***Abstract*—Power quality is a vital issue in the present power systems integrated with large renewable energy sources since more power electronics devices are incorporated in the system. This paper proposes a novel method for assessing power quality (PQ) associated with wind energy integration. This method is effective to recognize PQ issues in power systems with high penetration of wind energy with a low computational burden. Further, it detects different operational issues in the distribution network. Stockwell transform (S-transform) is utilized to decompose the voltage signal and calculate the S-matrix. To assess the PQ, a plot is developed from this matrix. The features of this matrix such as mean, standard deviation and maximum deviation are further utilized for detecting the operational issues such as wind speed variation, islanding, synchronization and outage of the wind generation by using clustering with Fuzzy C-means. A modified IEEE 13-bus test system is utilized to validate the proposed method which is also supported by hardware and real-time digital simulator (RTDS) results. The quality of power is graded with the help of a proposed power quality index under various operational events with different levels of wind energy penetration. The proposed method is effective for the identification and grading of different operational events in terms of PQ and recognizing a wide range of PQ issues with a high share of wind energy. The performance of the proposed scheme is established by comparing its results with other approaches.**

***Index Terms*—Grid synchronization, Fuzzy C-means clustering, Stockwell transform, islanding, outage, wind power.**

I. Introduction

WIND energy is treated as the fastest growing and most promising renewable energy (RE) resource around the world. According to the world wind energy association (WWEA), the wind industry is growing continuously worldwide with the overall installed capacity has touched to 597 GW by 2018 [1]. Various technical challenges such as stability, voltage regulation, reliability, protection and power quality (PQ) have become noticeable due to the integration of wind energy into the conventional electrical grid. Different PQ problems identified by the integration of wind energy are harmonic distortions, notch, voltage unbalance, voltage swell/sag, momentary interruptions, and flickers [2]. The PQ issues related to wind energy are determined by the measurement and standards of the International Electro-Technical Commission standard, IEC-61400 [3].

Power quality problems might lead to erratic operation of the electronic controllers and computer data loss. It might also lead to the mal-operation of relays, programmable logic controllers and computers [4]. For maintaining the electrical supply within the specified standards, it is required to monitor and mitigate the PQ disturbances. The features selection of the PQ disturbance, their localization, and classification decide the performance of mitigation techniques. The standard method of PQ issue (voltage events) detection is simple and easy to realize but unable to provide information related to the phase angle at the time of the event. Therefore, recognition and estimation of the PQ events are the key factors of the detection techniques. To effectively recognize the problems of PQ in the availability of renewable energy generation, artificial intelligence, and digital signal processing techniques are utilized nowadays [5]. The basic tool utilized for PQ analysis is short-time Fourier transform (STFT). Further, WT has been broadly utilized for analyzing stationary signals with their multi-resolution capability to cope up with STFT limitations [6]. Costa *et al.* [7], presented the methodology, which is based on the WT to characterize the voltage sags. For that purpose, voltage signals spectral energy is decomposed into wavelet and scaling coefficient energies. An integration of Gabor Transform (GT) and the Wigner distribution function (WDF) namely the Gabor-Wigner Transform (GWT) is utilized for detecting different PQ issues in [8]. A time-frequency spectral localization method namely Stockwell transform (S-transform) is combined with the properties of both WT and STFT. It utilized an analysis window with a minimized width that is based on the frequency and providing frequency-based resolution [9]. Kumar *et al.* [10], proposed a technique for recognizing single and multiple PQ problems. This technique relies on S-transform and utilized artificial intelligent classifier and rule-based decision tree (DT). Ray *et al.* [11], proposed a hyperbolic S-transform based classifier, employing support vector machine (SVM) and DT method to recognize and classify the PQ perturbations in the distributed generation systems. PQ analysis of the large wind energy generation plant, integrated with the practical distribution network of Taiwan has been presented in [12]. S-transform and WT are utilized for analysing the PQ disturbances and islanding detection of grid-integrated hybrid energy system comprising of solar

O. P. Mahela is with the Power System Planning Division, Rajasthan Rajya Vidhyut Prasaran Nigam Ltd., Jaipur-302005, India (email: opmahela@gmail.com)

B. Khan is with the Department of Electrical and Computer Engineering, Hawassa University, Hawassa, Ethiopia, 05 (email: baseem.khan04@gmail.com)

H. Haes Alhelou is with the Department of Electrical Power Engineering, Faculty of Mechanical and Electrical Engineering, Tishreen University, Lattakia 2230, Syria (email: alhelou@tishreen.edu.sy; h.haesalhelou@gmail.com)

P. Siano is with the Department of Management & Innovation Systems, University of Salerno, 84084 Salerno, Italy (email: psiano@unisa.it)

This article has been accepted for publication in a future issue of this journal, but has not been fully edited. Content may change prior to final publication. Citation information: DOI 10.1109/TII.2020.2971709, IEEE Transactions on Industrial Informatics

photovoltaic (PV), fuel cell and wind generator in [13]. Mahela *et al.* [14], proposed a WT based method for detecting and classifying PQ events, related to the wind energy integration. In [15], a S-transform and WT-based technique is suggested to detect the different PQ problems in grid-connected wind generation system.

The significant research contribution is reported to recognize PQ issues associated with the design of wind energy converters, the low penetration level of wind energy, water pumping system using wind energy etc. However, a small number of articles is available on PQ issues with wind energy penetration in the utility grid due to the operational events of wind power plants such as grid synchronization, outage, islanding and wind speed variations. Further, the performance of reported algorithms is quite low and affected by the presence of noisy signals. The proposed scheme overcomes these demerits.

This paper proposes a novel method based on Fuzzy C-means (FCM) clustering and S-transform, to detect problems of PQ related to wind energy integration with the utility grid and operational events. Different PQ issues discussed in this paper are islanding, wind speed variations, synchronization and disconnection of a wind generator to the grid. To cluster the data, the features extracted from the S-transform based decomposition of voltage signals are analyzed by using the Fuzzy C-means. Simulated results are validated with the help of RTDS and hardware setup of a grid integrated wind generator. For assessing the PQ with enhanced wind energy integration, the total harmonic distortions (THDs) of current and voltage waveforms and frequency variations are considered with the proposed new power quality index (PQI). The main contributions in this paper are as follows:

- Proposing a novel, technique based on Fuzzy C-means (FCM) clustering and S-transform to detect PQ disturbances associated with wind energy penetration into the utility grid and operational events.
- Proposing a computationally-efficient and noise-resistant method applicable to recognize a wide range of PQ events associated with the high wind energy penetration.
- The features extracted from the S-transform based voltage signal decomposition are fed to the Fuzzy C-means clustering for the clustering of the data.
- Validating the real-time implementation of the proposed method with the help of RTDS and a hardware set up of grid integrated wind generator.
- The proposed method is applicable to different practical cases in the industry such as islanding, wind speed variations, wind generator outage and synchronization issues.
- A novel power quality index (PQI) is proposed which is effective to identify various operational events in terms of PQ. Further, this PQI along with the power frequency variations and THD of voltage and current are utilized to assess the PQ with higher levels of wind energy (up to 60% in this work).

The paper is structured as follows. Section II introduces the test case system utilized to validate the proposed method. Section III details the proposed PQ detection technique and Section IV provides results and discussion. Section V presents the detection of operational events using Fuzzy C-means clustering. Implementation of the scheme for solar energy application is detailed in section VI. RTDS is employed to validate the simulation results in Section VII, while Section VIII includes hardware results. Section IX deals with performance comparison, followed by the conclusion.

II. Test System

The block-diagram of the modified grid-connected wind generator is illustrated in Fig. 1. It integrates a doubly-fed induction generation (DFIG) interfaced to an IEEE 13 bus test system utilizing grid and rotor side converters, filter and a transformer.

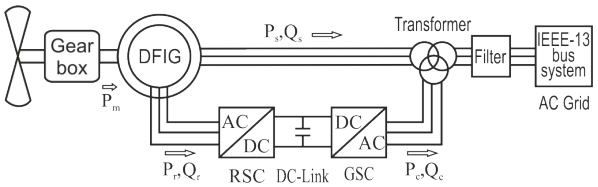

Fig. 1. Block diagram of proposed grid connected wind generator

A. wind energy system

The wind energy conversion system (WECS) consists of DFIG, run by a wind turbine. An adjustable speed induction generator (IG) and a wound rotor are consisted by DFIG. The advantages of IG include high energy output, minimization of the mechanical loads, less fluctuations in output power, easier pitch control, and a wide control range for both active and reactive powers [16]. The details related to the wind energy conversion system for the simulation are obtained from reference [17]. The DFIG's stator is coupled to the IEEE 13-bus power system through the transformer and filter whereas rotor side converters (RSC), grid side converters (GSC), DC link capacitor and a filter are utilized to connect rotor. Decoupled control of active and reactive powers of DFIG enabled by these converters [18]. The control for both RSC and GSC is Implemented using a proportional-integral (PI) controller based back-to-back pulse width modulation (PWM) converter. The wind turbines namely WG-1 and WG-2 are integrated with the IEEE 13 bus system at the buses 680 and 646, respectively. The capacities of both the wind turbines are equal and technical parameters are provided in the Appendix.

For performing the controlling actions, PI controller is utilized with the wind converters. As PI controller is utilized, more description is not added into the text as PI is the basic control strategy.

The PWM converters utilized at the grid and rotor side have the frequencies of 2700 Hz and 1620 Hz, respectively. Peak value of pitch angle is 27 degree with 10 degree/s maximum rate of variation. Gains of the pitch controller, voltage and reactive power regulators are 150, 20 and 0.05, respectively. Different values of the gains for Kp and Ki are given in the Appendix. Due to the limitation of the space and main focus on the wind generator operation, details of control techniques are not provided in the manuscript.

This article has been accepted for publication in a future issue of this journal, but has not been fully edited. Content may change prior to final publication. Citation information: DOI 10.1109/TII.2020.2971709, IEEE Transactions on Industrial Informatics

B. Proposed Modified Test System

A typical IEEE 13-bus power system is utilized in this work to accurately study the PQ disturbances and operational events related to the integration of the wind generation into the balanced distribution system.

The ratings of the standard system are as follows: 60Hz, 5MVA, two different voltage levels i.e. 0.48 kV and 4.16 kV with unbalanced and balanced demands. The standard system doesn't have any renewable energy (RE) source. The standard system is modified for integrating wind and diesel generators along with the balanced demands as shown in Fig. 2. The WG-1 is integrated at the bus 680 via transformer XWG-1 while WG-2 is integrated at the bus 646 via transformer XWG-2. The capacity of each wind generator used in the proposed study is 1.5 MW. Wind energy penetration level with the wind generation of capacities 1.5MW and 3MW are 30% and 60%, correspondingly. The capacity of the diesel generator is 3.125 MVA and it is connected at the bus 680 via transformer XDG. In this paper, two test cases are considered for investigating the impacts of wind energy on the quality of power. In the first case, power quality is investigated with WG-1 while in the second case simultaneously both the wind generators are integrated into the system.

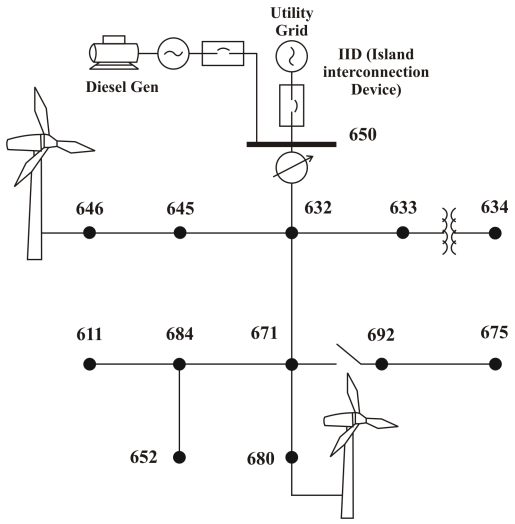

Fig. 2. Modified IEEE 13 bus test system

A spot load placed at the middle of the line is utilized to replace the distributed load between the buses 632 and 671. Modified loading and generator status of the IEEE 13-bus modified test system is presented in Table I. The three-phase overhead distribution line is utilized with the configuration of 601 to replace the 3-phase underground cable linking buses 692 and 675 along with the 1-phase underground cable situated amid buses 684 and 652. The impedances of selected overhead lines are similar as presented in the configuration 601 of the standard system. Equation (1) gives series impedance matrix of the feeders in Ohm/km. This matrix depends on the topology of the feeders and categories of the conductors [19].

A substation transformer is utilized to connect the feeder to the grid. The transformer XFM-1 is located between the nodes 633 and 634. The modified system omitted the voltage regulator connected amid the buses 650 and 632 from the original system.

$$Z_{601} = \begin{bmatrix} .2135 + 0.6235i & .0996 + .3171i & .0971 + .2623i \\ .0996 + 0.3247i & .2079 + .6521i & .0943 + .2329i \\ .0928 + 0.2362i & .0945 + .2932i & .2134 + .6403i \end{bmatrix} \quad (1)$$

TABLE I
THE STATUS OF LOADS AND GENERATORS [14]

Nodes	Load Model	Load		Capacitor	Generator
		kW	kVAr	(kVAr)	
634	PQ/Y	400	290	-	-
645	PQ/Y	170	125	-	-
646	PQ/Y	230	132	-	Wind-2
652	PQ/Y	128	86	-	-
671	PQ/Y	1155	660	-	-
675	PQ/Y	843	462	600	-
692	PQ/Y	170	151	-	-
611	PQ/Y	170	80	100	Diesel
632-671*	PQ/Y	200	116	-	-
680	-	-	-	-	Wind-1
650	-	-	-	-	Utility grid

⋆ The load between nodes 632 and 671 is exchanged by spot load located at middle of the line

A 3-phase circuit breaker is utilized for realizing the switch amid buses 671 and 692. The lengths of the lines are taken same as the standard system. An island interconnection device (IID) is used amid grid and bus 650 for realizing the islanded mode of test feeder.

III. Proposed Power Quality Recognition Method

Figure 3 presents the block diagram of the proposed methodology for detecting the power quality and operational issues. Voltage signals obtained from the bus 650 are sampled at the rate of 1.92 kHz i.e. 32 samples per cycle at 60 Hz. It is analyzed by utilizing S-transform for getting the output of complex S-matrix. Analysis of this matrix gives the information of PQ disturbances associated with the voltage signal. By adding the absolute values of each S-matrix's column, the suggested sum absolute values curve can be determined. This curve improves the output of the proposed method. ST plots used in the block diagram of Fig. 3 include the contour of frequency, the plots of amplitude, of the sum of absolute values, the plot of phase and of amplitude-frequency. Frequency contour and amplitude-frequency plots provide information on frequency variations and harmonics. However, plots of the amplitude and of the sum of absolute values provide information related to the variations in amplitude. Variations in amplitude of phase-time also indicate the presence of transient components. Further, it evidently presents the availability and allocation of each disturbance of PQ, that present in the waveform. Fuzzy C-means clustering is then used for detecting the various operational events by analyzing signals obtained from the sum absolute curves and S-matrix. Fast Fourier transform is used to compute overall harmonic distortions of voltage (THD_v) and current (THD_i). By constant observation of the system frequency, power frequency variations are also detected.

This article has been accepted for publication in a future issue of this journal, but has not been fully edited. Content may change prior to final publication. Citation information: DOI 10.1109/TII.2020.2971709, IEEE Transactions on Industrial Informatics

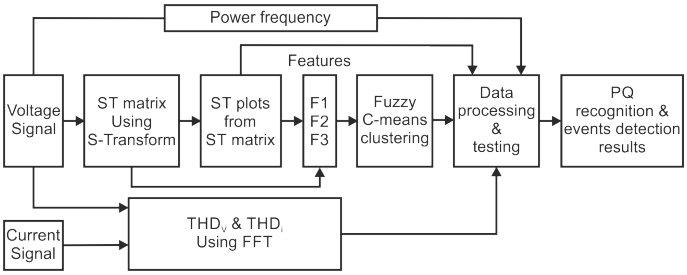

Fig. 3. Block scheme of PQ recognition and event detection

A. Stockwell Transform

The phase of the spectrum and amplitude contained the data associated with the PQ problems. The phase of the mother wavelet is updated for utilizing the data available in the phase of continuous wavelet transform (CWT).

$$W(\tau,a)=\int_{-\infty}^{\infty}h(t)\omega(t-\tau,a)dt \tag{2}$$

$\omega(t,d)$ denotes the fundamental mother wavelet scaled replica, d is dilation which defines the width of wavelet and regulates the resolution. The dilation factor is the inverse of frequency [13].

The WT of a function $h(t)$ is described as [9]

$$S(\tau,f)=e^{i2\pi ft}W(\tau,d) \tag{3}$$

where the mother wavelet can be determined as

$$w(t,f)=\frac{|f|}{\sqrt{2\pi}}e^{-\frac{t^2f^2}{2}}e^{-i2\pi ft} \tag{4}$$

The explicit form of S-transform is given as

$$S(\tau,f)=\int_{-\infty}^{\infty}h(t)\frac{|f|}{\sqrt{2\pi}}e^{-\frac{(\tau-t)^2f^2}{2}}e^{-i2\pi ft}dt \tag{5}$$

The disturbance signal of the power system $h(t)$ can be formulated using discrete-time series as $h[kT], k=0,1,...,N-1$, in which T is the sampling time and N is the number of samples. The discrete form of Fourier transform can be applied to the time-series $h(t)$ that results in [20]

$$H\left[\frac{n}{NT}\right]=\frac{1}{N}\sum_{k=0}^{N-1}h[kT]e^{\frac{-i2\pi nk}{N}};\ \ n=0,1,...,N-1 \tag{6}$$

The S-transform is defined as the vectors projection shown by the time series $h[kT]$ onto vectors' spanning set. The S-transform explicit form of a discrete-time series $h[kT]$ is mathematically defined as (letting $f\rightarrow n/NT$ and $\tau\rightarrow jT$) [9]

$$S\left[jT,\frac{n}{NT}\right]=\sum_{m=o}^{N-1}H\left[\frac{m+n}{NT}\right]e^{-\frac{2\pi^2m^2}{n^2}}e^{\frac{i2\pi mj}{N}};n\neq 0 \tag{7}$$

if $n=0$ voice, then S-transform can be reformulated as follows

$$S\left[jT,0\right]=\frac{1}{N}\sum_{m=o}^{N-1}H\left[\frac{m}{NT}\right] \tag{8}$$

The S-transform output is calculated as a complex matrix $(N\times M)$ known as the S-matrix. In this matrix, rows and columns correspond to the definite frequencies and times, respectively. The S-matrix amplitude and phase can be determined as $|S\left[jT,n/NT\right]|$, and $tan^{-1}(imag(S\left[jT,n/NT\right])/real(S\left[jT,n/NT\right]))$, respectively.

B. FCM Clustering Technique

FCM is a multiple clustering method that is first suggested by Dunn and later generalized by Bezdek in [21]. In this technique, the basic C-Means functions or its variations are optimized. The objective function is described as

$$J_m=\sum_{i=1}^{N}\sum_{j=1}^{C}u_{ij}^m||x_i-c_j||^2 \tag{9}$$

where m, x_i, u_{ij}, and c_j are to the clusters number, the i_{th} element of n-dimensional measured data, the membership degree of x_i in cluster j, and the n-dimensional center of the cluster.

FCM has the ability to calculate, and in turn, iteratively update the data point values of membership function with the clusters pre-defined number. Therefore, the data point can be a member of all clusters with corresponding membership values [22].

C. Power Quality Index

Depend on the various calculated factors such as maximum change in the sum absolute values curve and amplitude, frequency fluctuation, THD_v, THD_i, a novel power quality index (PQI) is developed to rate the operational issues of DFIG, such as islanding and wind speed variations, from the power quality point of view. Furthermore, the PQI considers the time duration of the PQ disturbances, and it is described as follows

$$PQI=\left(\frac{\alpha|\Delta A|t_1+\beta|\Delta S|t_2+\gamma|\Delta f|t_3+\delta THD_v+\sigma THD_i}{5}\right)*100 \tag{10}$$

where ΔA represents the maximum deviation in the amplitude plot of S-transform, ΔS represents the maximum variation in the sum absolute values plot of S-transform, Δf represents the maximum deviation in electrical frequency, THD_i and THD_v represent fractional THDs of current and voltage, respectively. t_1, t_2, and t_3 represent the duration for which the perturbations in magnitude, sum absolute values curve and electrical frequency persists. $\alpha,\beta,\gamma,\delta$, and σ indicts the weights associated with the magnitude, sum absolute values, electrical frequency, THD_v, and THD_i, correspondingly. Here, ΔA and ΔS include the information extracted from the output S-matrix obtained by the decomposition of voltage signal using the Stockwell transform.

A higher value of PQI shows that the power quality of the grid is severely affected. PQI quantifies the power quality events inversely proportional to its value. The selection of weights is depended on the deterioration in the supply quality and its value varied from zero to any positive value. In this

This article has been accepted for publication in a future issue of this journal, but has not been fully edited. Content may change prior to final publication. Citation information: DOI 10.1109/TII.2020.2971709, IEEE Transactions on Industrial Informatics

paper, $\alpha, \beta, \gamma, \delta$, and σ are selected unity to detect the PQ disturbances related to the deviations in frequency, amplitude variations and availability of harmonics in both the current and voltage signals. However, these weights may have different values depending on the type of the case study.

D. Advantages of Proposed Scheme

The main advantages of the proposed schemes are:

- This scheme is effective in recognition of PQ disturbances with different natures related to variations in magnitude, frequency, harmonics, transients etc. even with the high penetration level of wind energy. This is achieved in the present study with 60% wind energy penetration level.
- This scheme can be used invariably with wind and solar energy penetration into the utility grid. Hence, it can be used for monitoring the PQ in present-day utility networks with RE penetration.
- This scheme is based on S-transform, hence it gives a frequency-dependent resolution of time, frequency and phase, which makes the algorithm effective for the identification of a wide range of PQ disturbances.
- The performance of this scheme is least affected by the noise.
- The proposed PQ index is effective in the detection of the different operational events of wind energy in terms of the level of PQ disturbances. It is also effective to investigate the effect of increased penetration level on the quality of power.

IV. Simulation Results and Discussion

Results obtained from the detection of PQ disturbances related to the outage and synchronization of the wind generator is discussed in this section. Furthermore, PQ disturbances related to the islanding and wind velocity deviation are also investigated in this section. PQ problems are analyzed by employing different S-transform based curves obtained from the S-matrix and frequency contents of the signal. Normalization of the parameters is performed with reference to their maximum values. These curves are compared to the corresponding curves of standard PQ disturbances [23].

A. Wind Generator Grid Synchronization

The synchronization of the $1.5MW$ rated capacity wind generator to the grid is done at 0.33 second and corresponding S-transform depended curves are presented in Fig. 4. From the curves, it is clear that the PQ transients sustained for the duration of 3 seconds. Voltage variations such as sag and swell can be monitored from the amplitude curve depicted in Fig. 4 (b). Voltage sag is developed at the time of grid synchronization of wind turbine because the inrush current is drawn from the grid by the wind turbine generator. This reverses the power flow towards the wind generator due to which a voltage swell is created, which ultimately leads to the voltage fluctuations. These voltage fluctuations are the source of flickers. Sum absolute values curve, which is presented by Fig. 4 (c), shows the voltage sag and swell. The isolated contour in Fig. 4 (a) specified the existence of oscillatory transient (OT). The sudden changes in the phase plot of Fig. 4 (d) also specified the existence of transients at the time of wind generator synchronization. Finite values amid the normalized frequency range of 0.08-0.3 in the amplitude-frequency plot given in Fig. 4 (e) which indicates the existence of harmonics of various frequencies. Voltage in the system also increased approximately by 0.02 pu at the time of wind turbine integration due to injection of the real power. Further, it is clear from the curves that the amount of detected PQ disturbances raises with the penetration of wind energy level to $3MW$ as compared to the $1.5MW$. S-transform based plots of $3MW$ wind generator is only presented in this manuscript due to space restrictions.

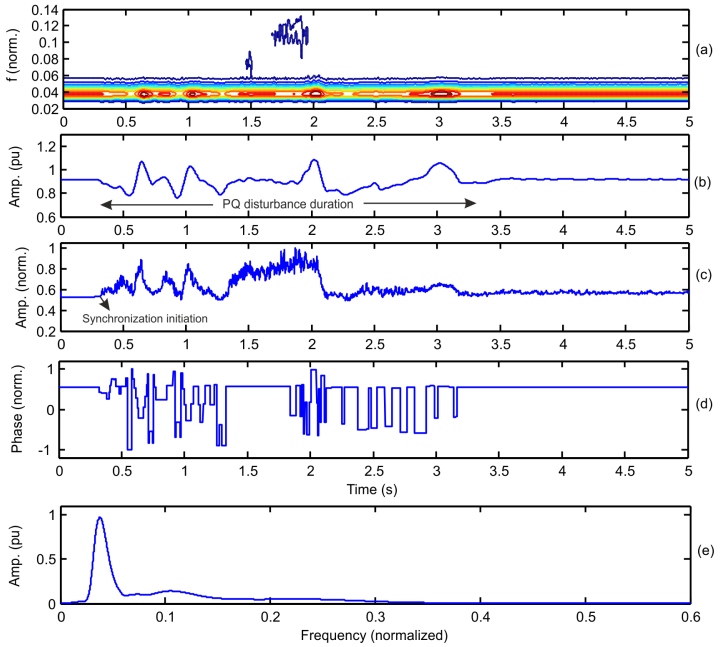

Fig. 4. Results (a) contour of frequency (b) plot of amplitude-time (c) plot of the sum absolute values (d) plot of phase-time (e) plot of amplitude-frequency of S-transform for grid synchronization of wind generator.

Power frequency at the time of grid integration of wind generator is presented in Fig. 5. Frequency variations for a period of 3.5 seconds are observed following the grid synchronization. Frequency varies between $60.5Hz$ to $59.7Hz$ with wind energy penetration of 3MW whereas frequency varies between $60.2Hz$ to $59.9Hz$ with wind generator of capacity $1.5MW$. Thus the frequency deviations increase with the wind energy penetration level. Frequency quality is greatly degraded by the high wind power share. Table II presents the values of THD_v and THD_i with wind energy integrations of capacities of $1.5MW$ and $3MW$ during transient duration. From Table II, it can be seen that the harmonics distortion level in the grid rises with the wind energy integration.

B. Wind Generator Outage

At 0.33 second the outage of a wind generator is simulated in this work. Active power supplied by the wind turbine to the utility decreases suddenly to zero during the outage event.

This article has been accepted for publication in a future issue of this journal, but has not been fully edited. Content may change prior to final publication. Citation information: DOI 10.1109/TII.2020.2971709, IEEE Transactions on Industrial Informatics

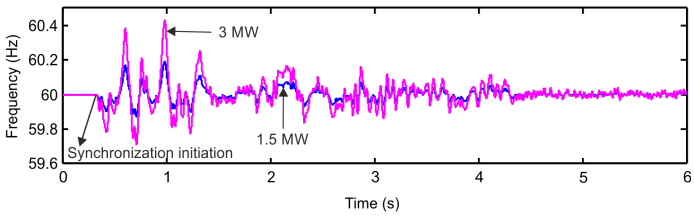

Fig. 5. Frequency variations during grid synchronization of wind generators.

TABLE II
VOLTAGE AND CURRENT THD

S.	study cases	THD_v (%)		THD_i (%)	
		$1.5MW$	$3MW$	$1.5MW$	$3MW$
1	Grid synchronization of WG	0.06	0.67	11.71	24.04
2	Outage of wind Gen.	1.15	7.61	16.03	19.54
3	Islanding	3.50	8.68	18.94	28.11
4	Wind speed variations	1.03	2.79	15.79	24.12

PQ disturbances are faced by the utility grid due to this sudden outage. Figure 6 presents the S-transform curves of voltage waveforms for phase A during wind turbine outage. Availability of impulsive transient (IT) is shown by the sharp magnitude peak presented in the sum absolute values plot in fig. 6 (C), abrupt variation observed in the phase plot of fig. 6 (d) and a low magnitude variation presented in the S-contour at 0.33 second of Fig. 6 (a). Fig. 6 (c) shows the low amount of ripples in the sum absolute values curve after the outage of short duration. Availability of harmonics is confirmed by the finite values of normalized frequencies between the values of 0.1 to 0.22 in frequency amplitude curve of Fig. 6 (e). Voltage magnitude slightly increased after the outage by a value of 0.02 p.u because reactive power is reduced after the outage of induction generator.

Fig. 7 introduces the power frequency waveform at the outage of wind generator. A sudden drop in the frequency from $59.95Hz$ and $59.82Hz$ occurs after the outage of wind generators at rated capacities of $1.5MW$ and $3MW$, respectively. After the duration of 0.05 second, frequency is resorted. Small changes in the amplitudes of frequency are observed at the time of resorting of the original value of frequency. Values of THD_v and THD_i with the outage of wind generation of capacities 1.5 MW and 3 MW are provided in Table II. High wind energy penetration increases the frequency deviations as well as THD_v and THD_i with the outage of wind turbines.

C. Islanding

Islanding of the test system from the grid in the availability of $3MW$ of WG-1 and WG-2 generators is simulated at 0.33 second. At the time of islanding, XDG will automatically turn on. The test network is operated as a micro-grid. The diesel generator supplies the reactive power drawn by the DFIG. The wind and diesel generators supply active power to the loads. Fig. 8 (b) and (c) presented the voltage fluctuations, sag and swell with the help of amplitude and sum absolute values plots. Variations in the voltage persist for duration of 2.2 second. These voltage variations produce the flicker. The presence of harmonics can be detected by the finite values

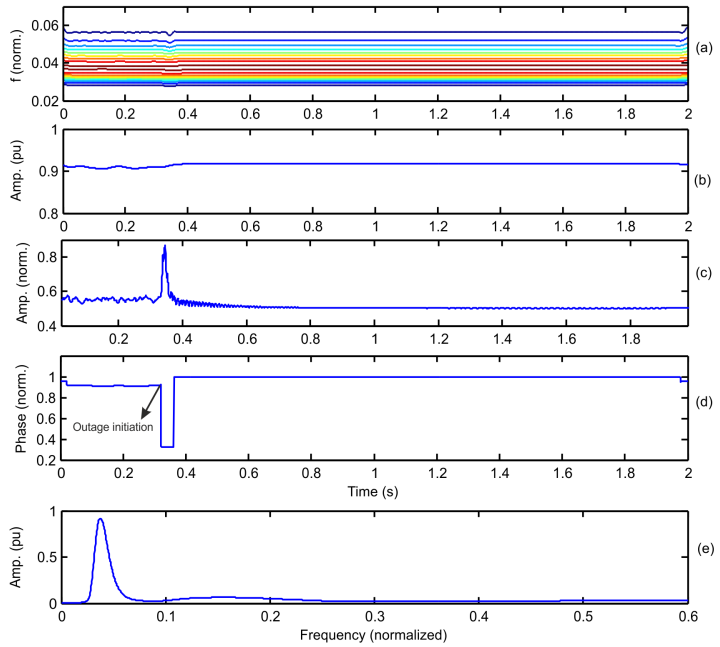

Fig. 6. Results: a) contour of frequency; b) amplitude-time curve; c) plot of sum of absolute values; d) curve of phase-time; and e) plot of amplitude frequency of S transform in case of outage

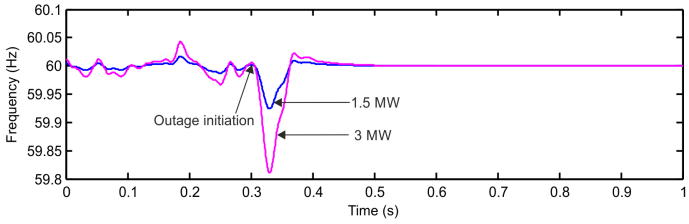

Fig. 7. Frequency during outage of wind generators.

of the normalized frequencies between the ranges of 0.08 to 0.25 in the plot of frequency-amplitude curve of Fig. 8 (e). Availability of OT is presented by the isolated upper contours available in the S-contour of Fig. 8 (a). Moreover, the large variations in the phase plot presented by Fig. 8 (d) indicated the availability of OT. A transient over-voltage followed by islanding operation has to be handled properly in the micro-grid operation.

The changes in the frequency at the time of islanding are shown in Fig. 9. With one wind generator of capacity $1.5MW$ integrated with the test network, the frequency first increases to $65Hz$ and later starts decreasing continuously since the generation is less than the demand. The power system network becomes unstable due to mismatch in the load and supplied power, which ultimately lead to shutting down of the microgrid operation. With the $3MW$ of wind energy generation, the frequency first increases to a value of $64Hz$ and finally reaches to a value of $60Hz$ resulting in stable operation as a microgrid. This is due to the fact that the generation capacity matches the load demand. The values of THD_v and THD_i during islanding event with wind energy penetration levels of $1.5MW$ and $3MW$ are provided in Table II. It is clear from the table

This article has been accepted for publication in a future issue of this journal, but has not been fully edited. Content may change prior to final publication. Citation information: DOI 10.1109/TII.2020.2971709, IEEE Transactions on Industrial Informatics

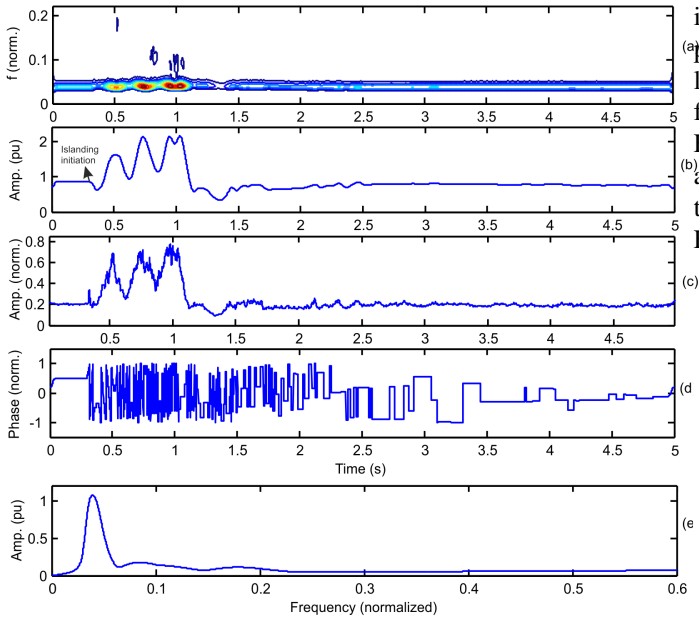

Fig. 8. Obtained results: a) contour of frequency; b) plot of amplitude and time; c) plots of sum absolute values; d) plot of phase and time; and e) plot of amplitude and frequency for S-transform of islanding of test system with diesel and wind generators

that with the increase in wind energy penetration level into the grid, the level of harmonic distortion is also increased.

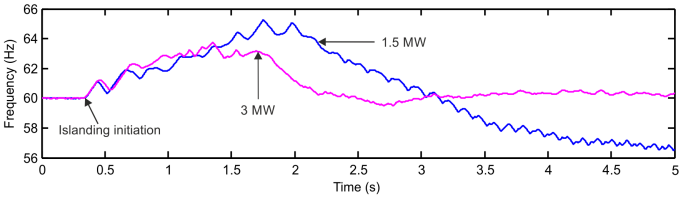

Fig. 9. Frequency during islanding event.

D. Wind Speed Variations

The simulated wind speed variations for a period of 2 second are shown in Fig. 10. Abrupt changes in wind speed are simulated for finding the highest impact of wind speed variations on the power quality.

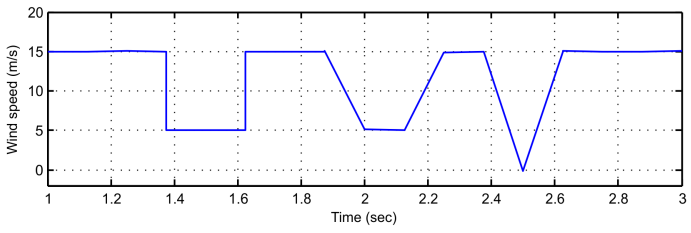

Fig. 10. Wind speed variations.

Fig.11 presents the S-transform depended one voltage waveform curves with the wind speed variations. Variations in wind speed are responsible for the input mechanical torque fluctuations to the generator. This resulted in voltage fluctuations in the utility grid, which is visible in the amplitude curve presented by Fig. 11. These voltage fluctuations produced a low magnitude flicker. The non-zero values of normalized frequencies between 0.08 and 0.25 which is presented by Fig. 11 (e) of the frequency-amplitude curve showed the availability of harmonics. The availability of low magnitude transients are indicated by the variations in the phase curve of Fig. 11 (d).

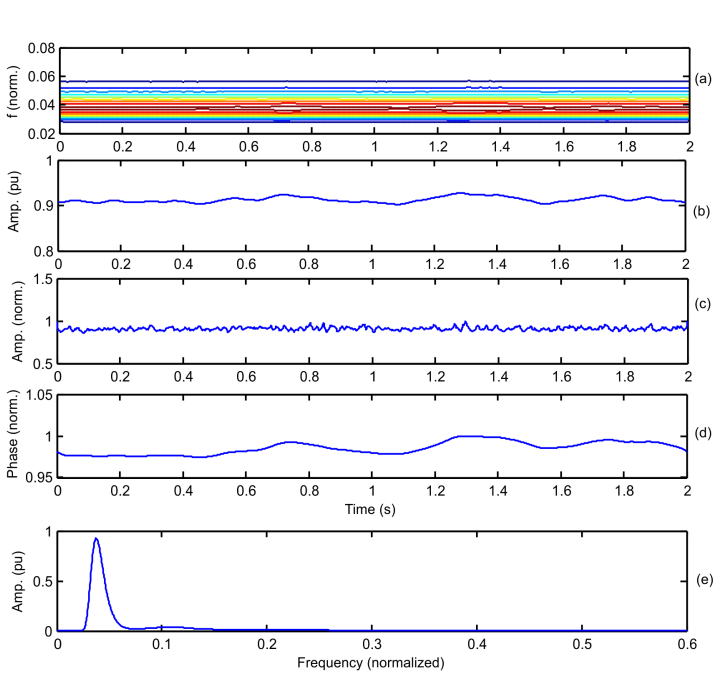

Fig. 11. Results: a) contour of frequency; b) plot of amplitude- tine; c) plots of sum absolute values; d) plot of phase- time; and e) plot of amplitude-frequency for S-transform of wind speed variations

Frequency during wind speed variations is shown in Fig. 12. The variations of small magnitude between the frequencies $59.98Hz$ and $60.02Hz$ are observed due to the wind speed variations in the presence of wind generator of capacity $1.5MW$. However, the frequency varies between $59.96Hz$ and $60.04Hz$ in the presence of wind energy generation of capacity $3MW$. Hence, it has been observed that power frequency is not affected significantly even due to drastic change in the wind speed. Values of THD_v and THD_i with the variations in wind speed are provided in Table II, from which it can be established that the wind energy penetration level increases the values of THD_v and THD_i. It is also established that the frequency deviations also increase with the wind energy penetration level.

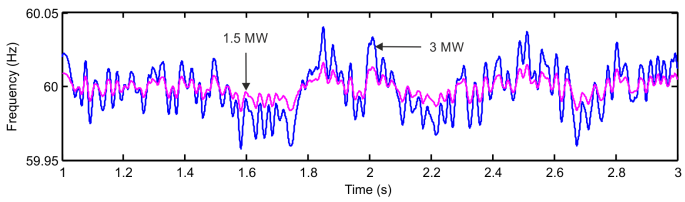

Fig. 12. Frequency during wind speed variations.

This article has been accepted for publication in a future issue of this journal, but has not been fully edited. Content may change prior to final publication. Citation information: DOI 10.1109/TII.2020.2971709, IEEE Transactions on Industrial Informatics

Table III provided the maximum variations in power frequency from the rated $60Hz$ of the studied system integrated with wind generation of capacities $1.5MW$ and $3MW$ for the duration of all the events. From Table III, it is clear the highest variation in the frequency is found at the time of islanding, which is followed by the synchronization, outage and wind speed variations, respectively. Furthermore, with the increase in wind energy penetration to the grid, frequency deviations also increased.

TABLE III
MAXIMUM FREQUENCY DEVIATIONS WITH WIND ENERGY PENETRATION

S.	Event description	Class symbol	Frequency deviation (Hz)	
			$1.5MW$	$3MW$
1	Grid synchronization of WG	E1	0.200	0.500
2	Outage of wind Gen.	E2	0.050	0.180
3	Islanding	E3	3.105	4.080
4	Wind speed variations	E4	0.020	0.038

Table IV introduces the various PQIs calculated for the events selected with this study with the wind generation capacities of $1.5MW$ and $3MW$. It is clear that the overall power quality is severely affected by the islanding, which is followed by the synchronization, variation in the wind speed and outage. It is further observed that the power quality deteriorated with the level of wind energy penetration, respectively.

TABLE IV
POWER QUALITY INDEX

S.	Event description	Power quality index	
		$1.5MW$	$3MW$
1	Grid synchronization of WG	19.082	57.684
2	Outage of wind generator	4.125	9.728
3	Islanding	517.281	357.576
4	Wind speed variations	8.519	12.642

V. FUZZY C-MEANS CLUSTERING UTILIZATION FOR OPERATION EVENTS DETECTION

With the utilization of the proposed Fuzzy C-means clustering, various operational events such as islanding, wind speed variations, outages, and grid synchronization can be accurately detected. Three features labeled as F1, F2 and F3 are extracted from the time frequency plot of the voltage signal by using the suggested S-transform and are utilized for detecting and classifying the various operational events. These features are as follows

- **F1**: Mean

$$F1 = mean(abs(S(j,n))) \tag{11}$$

- **F2**: Standard deviation

$$F2 = std(abs(S(j,n))) \tag{12}$$

- **F3**: Maximum deviation

$$F3 = max(Smatrix) - F1 \tag{13}$$

The F2-time and F3-time scatter plots are found to be effective to detect operation events such as islanding, wind speed variations, grid synchronization and outage of wind generators. Fig. 13 depicts the scatter plots of F2-time and F3-time which separates various events investigated by clustering the data.

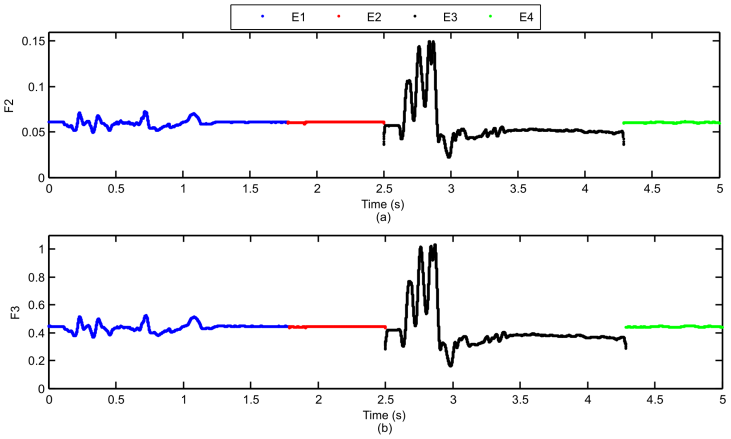

Fig. 13. Detection of operational events using FCM (a) feature $F2$ versus time and (b) feature $F3$ versus time scatter plots.

The scatter plots showed in Fig. 13 are useful to detect the PQ events. It is clear from the above that the PQ events, i.e. voltage sag, swell, fluctuations, are associated with the operational events such as wind speed variations, synchronization and islanding. Furthermore, outage of generator is related to voltage swell.

VI. VALIDATION OF THE RESULTS FOR REAL-TIME IMPLEMENTATIONS

The real-time digital simulator (RTDS) of OPAL-RT is utilized to validate simulation results calculated in this work. RTDS is interfaced with the human interface device (HID). The configuration of the host laptop utilized as HID has 64 bit operating system, 4 GB RAM, Intel (I) Core(TM) i5-3230M CPU@2.60 GHz processor. MATLAB/Simulink 2011b software environment is utilized to model test system on HID and uploaded on ML605 target of RTDS. OpWrite Block of the RT-Lab is utilized to take out the data and plotted with the help of MATLAB plot window. It is worth mentioning that the ether-net communication system is adopted to perform the communication between host laptop and RTDS system.

Fig. 15 presented the S-transform depended on curves of real-time results calculated from RTDS in the event of outage. These real-time results are closely matched with the simulation results shown in Fig. 6. These results clearly validate the real-world implementation of the proposed method.

Power quality index with respect to the real time result is calculated to show the accuracy of the simulation results. The index shown in (14) is utilized to calculate the percentage error, E, for the simulation results.

$$Er = (\frac{S-R}{R}) * 100\% \tag{14}$$

where S, and R are the simulation and real-time results, respectively. A comparison between simulation and real-time results are presented in table V. From the table, it is clear

This article has been accepted for publication in a future issue of this journal, but has not been fully edited. Content may change prior to final publication. Citation information: DOI 10.1109/TII.2020.2971709, IEEE Transactions on Industrial Informatics

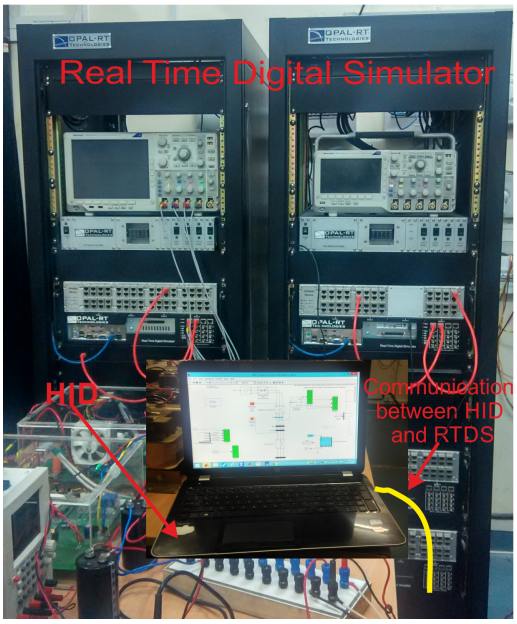

Fig. 14. Experimental platform used for implementing the proposed method

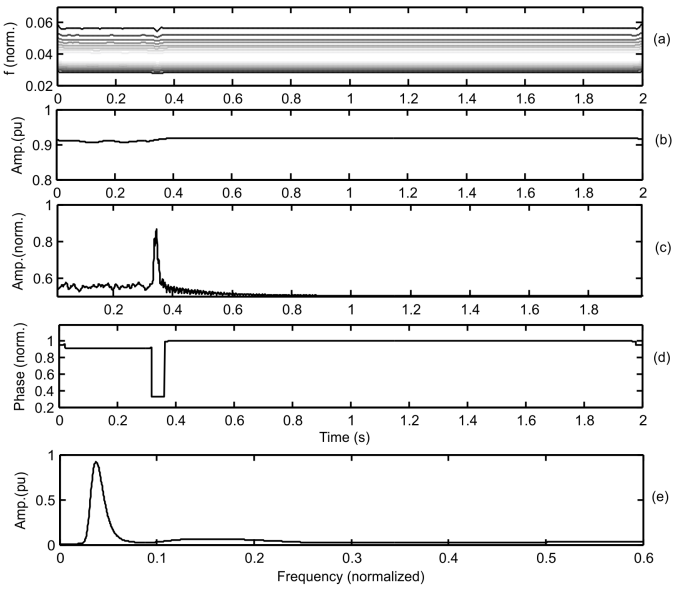

Fig. 15. Results obtained from real-time implementation: (a) Contour of frequency; (b) plot of amplitude-time; (c) plots of sum absolute values; (d) plot of phase-time; and (e) plot of amplitude-frequency for S-transform of outage of wind generator

that the maximum error is less than 2%. Therefore, to assess the power quality and detecting the various operational events, the proposed S-transform depended methods can be efficiently employed in the distribution network with a high share of wind energy integration.

VII. Hardware Validation of Results

Experimental validation of results has been performed using a DFIG based wind power plant rated at 0.8kW, 230 V, 50 Hz and 1500 rpm integrated to a distribution network operating at 400 V, 50 Hz in Jodhpur, India. A three-phase load comprising of a series combination of 600 W resistive load and 0.45 H, 1.8Ω, 330 turns inductance in each phase is used as RL load. A delta connected 3-phase, 10 W, 50 Hz, 415 V, 1430 rpm induction motor is used to see the effects of motor load. The block scheme is the same as shown in Fig. 2. An outage of a wind generator is performed at 0.095s and recorded voltage is processed using the proposed method. Fig. 16, shows the voltage waveform and S-transform based plots. Impulsive transient (IT) is detected by a sharp magnitude peak observed at 0.095 seconds in sum absolute values curve of Fig. 16 (d). The presence of harmonics has been confirmed by the finite values of the frequency-amplitude curve of Fig. 16 (d). Hence, hardware results are in line with the simulation results. The values of THD_v, THD_i, frequency deviations and PQ index for the outage of a wind generator in the presence of inductive and motor loads are tabulated in Table VI. It is evident that the parameters are also in line with the simulation results. It is also observed that the presence of inductive load affects the quality of power more adversely compared to the induction motor.

TABLE V
Comparison of Power Quality Index (1.5 MW) Results in Case of Real-Time Implementation

Event description	PQI		Percentage deviation (%)
	Simulation	Real Time	
Grid synchronization of WG.	19.082	18.815	1.4191
Outage of wind generator	4.125	4.079	1.1152
Islanding	517.281	516.592	0.1334
Wind speed variations	8.519	8.394	1.4892

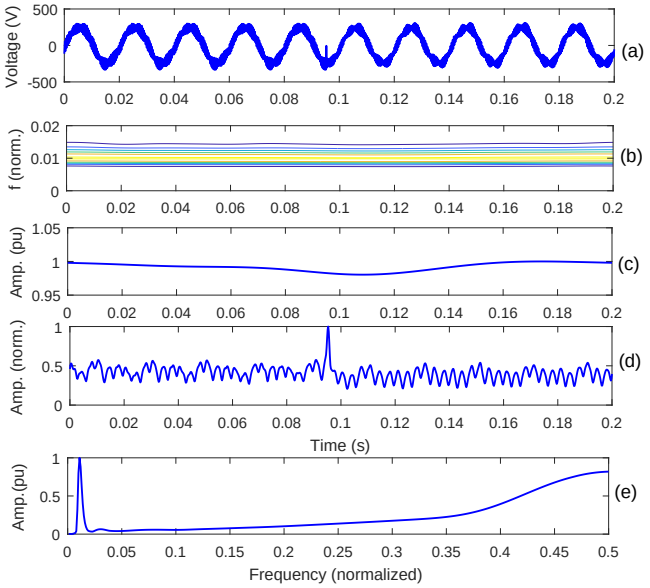

Fig. 16. Hardware results: (a) Voltage waveform; (b) contour of frequency; (c) plot of amplitude-time; (d) plots of sum absolute values; and (e) plot of amplitude-frequency for S-transform of an outage of a wind generator with induction motor load

TABLE VI
HARDWARE RESULTS CONSIDERING AN OUTAGE OF WIND GENERATOR

S. No.	Type of Load at PCC	THD_v	THD_i	Frequency deviation	PQ index
1	Inductor load	1.5608	2.6473	0.0327	4.4040
2	Induction motor	1.5851	2.3073	0.0319	2.7066

VIII. CONCLUSIONS

To evaluate the power quality events and detect the operation events in the distribution system with high wind energy penetration, this paper proposed a novel algorithm. Multi resolution analysis based S-transform is utilized to analyze the voltage signal for developing various curves for power quality assessment. The events under the investigation include islanding, synchronization, outage and wind speed variations. The power quality disturbances under each event are recognized precisely. The proposed PQI is used to evaluate the quality of power during various events with different wind energy penetration levels. It is clear from the results that the overall quality of power is severely affected during the islanding event, which is followed by the synchronization, wind speed variation and outage. Moreover, an increase in the penetration of wind energy, decrease the power quality. For fuzzy C-means clustering, three features are extracted from the S-matrix and employed for detecting the various operational events. RTDS is utilized to verify the accuracy of the simulation results. Results are also validated using hardware set up of grid-connected wind generator. The performance of proposed schemes is compared wit WT based scheme and found superior. Therefore, for assessing the power quality and detecting the various operational events, the proposed S-transform depended method can be efficiently employed in the real-world distribution system with a high level of wind energy share.

IX. APPENDIX

A- Technical parameters of wind energy conversion system are as follows:

f= 60 Hz; P= 1500 kW; V=575 V; Nominal wind sped (v)= 11 m/sec; H= 0.675 sec; Inductances of rotor and stator are 0.15 and 0.19 p.u, respectively; per unit; Resistances of stator and rotor are 0.695 and 0.17 p.u, respectively; and Coupling (mutual) inductance= 2.89 per unit.

B- Controllers' parameters:

Voltage controller of Dc bus (kp=9.0 & ki=450); Current controller in the grid-side converter (kp=0.91 & ki=8.0); Current controller in rotor side converter (kp=0.90 & ki=7.0); Speed regulator (kp=4.0 & ki=0.7); and Compensator gains for pitch angle (kp=4.0 & ki=29).

C- The details of various transformers utilized in the test system are omitted due to space limitation.

REFERENCES

[1] M. Moness and A. M. Moustafa, "Real-time switched model predictive control for a cyber-physical wind turbine emulator," *IEEE Transactions on Industrial Informatics*, 2019.

[2] M. Rostami and S. Lotfifard, "Optimal remedial actions in power systems considering wind farm grid codes and upfc," *IEEE Transactions on Industrial Informatics*, 2019.

[3] F. Chishti, S. Murshid, and B. Singh, "Lmmn based adaptive control for power quality improvement of grid intertie wind-pv system," *IEEE Transactions on Industrial Informatics*, 2019.

[4] M. Babakmehr, H. Sartipizadeh, and M. G. Simoes, "Compressive informative sparse representation-based power quality events classification," *IEEE Transactions on Industrial Informatics*, 2019.

[5] M. Sahani and P. K. Dash, "Fpga-based online power quality disturbances monitoring using reduced-sample hht and class-specific weighted rvfln," *IEEE Transactions on Industrial Informatics*, vol. 15, no. 8, pp. 4614–4623, 2019.

[6] W.-M. Lin, C.-H. Wu, C.-H. Lin, and F.-S. Cheng, "Detection and classification of multiple power-quality disturbances with wavelet multiclass svm," *Power Delivery, IEEE Transactions on*, vol. 23, no. 4, pp. 2575–2582, Oct 2008.

[7] F. B. Costa and J. Driesen, "Assessment of voltage sag indices based on scaling and wavelet coefficient energy analysis," *Power Delivery, IEEE Transactions on*, vol. 28, no. 1, pp. 336–346, Jan 2013.

[8] C. Soo-Hwan, G. Jang, and S.-H. Kwon, "Time-frequency analysis of power-quality disturbances via the gabor-wigner transform," *Power Delivery, IEEE Transactions on*, vol. 25, no. 1, pp. 494–499, Jan 2010.

[9] R. G. Stockwell, L. Mansinha, and R. P. Lowe, "Localization of the complex spectrum: the s transform," *Signal Processing, IEEE Transactions on*, vol. 44, no. 4, pp. 998–1001, Apr 1996.

[10] R. Kumar, B. Singh, D. T. Shahani, A. Chandra, and K. Al-Haddad, "Recognition of power-quality disturbances using s-transform-based ann classifier and rule-based decision tree," *Industry Applications, IEEE Transactions on*, vol. 51, no. 2, pp. 1249–1258, March 2015.

[11] P. K. Ray, S. R. Mohanty, N. Kishor, and J. P. S. Catalao, "Optimal feature and decision tree-based classification of power quality disturbances in distributed generation systems," *Sustainable Energy, IEEE Transactions on*, vol. 5, no. 1, pp. 200–208, Jan 2014.

[12] C.-T. Hsu, R. Korimara, and T.-J. Cheng, "Power quality analysis for the distribution systems with a wind power generation system," *Computers and Electrical Engineering*, vol. 54, pp. 131 – 136, 2016.

[13] P. K. Ray, N. Kishor, and S. R. Mohanty, "Islanding and power quality disturbance detection in grid-connected hybrid power system using wavelet and s -transform," *Smart Grid, IEEE Transactions on*, vol. 3, no. 3, pp. 1082–1094, Sept 2012.

[14] O. P. Mahela and A. G. Shaik, "Power quality detection in distribution system with wind energy penetration using discrete wavelet transform," in *Advances in Computing and Communication Engineering (ICACCE), 2015 Second International Conference on*, May 2015, pp. 328–333.

[15] P. K. Ray, H. C. Dubeya, S. R. Mohanty, N. Kishor, and K. Ganesh, "Power quality disturbance detection in grid-connected wind energy system using wavelet and s-transform," in *Power, Control and Embedded Systems (ICPCES), 2010 International Conference on*, Nov 2010, pp. 1–4.

[16] S. Li, T. A. Haskew, and J. Jackson, "Integrated power characteristic study of {DFIG} and its frequency converter in wind power generation," *Renewable Energy*, vol. 35, no. 1, pp. 42 – 51, 2010.

[17] O. P. Mahela and A. G. Shaik, "Comprehensive overview of grid interfaced wind energy generation systems," *Renewable and Sustainable Energy Reviews*, vol. 57, pp. 260 – 281, 2016.

[18] D. Ehlert and H. Wrede, "Wind turbines with doubly-fed induction generator systems with improved performance due to grid requirements," in *Power Engineering Society General Meeting, 2007. IEEE*, June 2007, pp. 1–7.

[19] O. P. Mahela and A. G. Shaik, "Power quality recognition in distribution system with solar energy penetration using s-transform and fuzzy c-means clustering," *Renewable Energy*, vol. 106, pp. 37 – 51, 2017.

[20] I. W. C. Lee and P. K. Dash, "S-transform-based intelligent system for classification of power quality disturbance signals," *Industrial Electronics, IEEE Transactions on*, vol. 50, no. 4, pp. 800–805, Aug 2003.

[21] T. C.-K. Huang, W.-H. Hsu, and Y.-L. Chen, "Conjecturable knowledge discovery: A fuzzy clustering approach," *Fuzzy Sets and Systems*, vol. 221, pp. 1 – 23, 2013, theme: Clustering.

[22] B. Biswal, H. S. Behera, R. Bisoi, and P. K. Dash, "Classification of power quality data using decision tree and chemotactic differential evolution based fuzzy clustering," *Swarm and Evolutionary Computation*, vol. 4, pp. 12 – 24, 2012.

[23] O. P. Mahela and A. G. Shaik, "Recognition of power quality disturbances using s-transform and fuzzy c-means clustering," in *2016 International Conference on Cogeneration, Small Power Plants and District Energy (ICUE)*, Sept 2016, pp. 1–6.